Inorg. Chem. **2008**, *47*, 1044–1052

Toward Multifunctional Mo(VI–IV) Complexes: *cis*-Dioxomolybdenum(VI) Complexes Containing Hydrogen-Bond Acceptors or Donors

Lyndal M. R. Hill, Michelle K. Taylor, Victor Wee Lin Ng, and Charles G. Young*

School of Chemistry, University of Melbourne, Victoria 3010, Australia

Received October 4, 2007

The complexes *cis*-Tp$^{i\mathrm{Pr}}$Mo$^{\mathrm{VI}}$O$_2$(OAr-R) (Tp$^{i\mathrm{Pr}}$ = hydrotris(3-isopropylpyrazol-1-yl)borate, $^-$OAr-R = hydrogen-bonding phenolate derivative) are formed upon reaction of Tp$^{i\mathrm{Pr}}$MoO$_2$Cl, HOAr-R, and NEt$_3$ in dichloromethane. The orange, diamagnetic, dioxo–Mo(VI) complexes exhibit strong ν(MoO$_2$) IR bands at ca. 935 and 900 cm^{-1} and NMR spectra indicative of C_s symmetry. They undergo electrochemically reversible, one-electron reductions at potentials in the range –0.836 to –0.598 V vs SCE; the only exception is the 2-CO$_2$Ph derivative, which exhibits an irreversible reduction at –0.924 V. The complexes display distorted octahedral geometries, with a cis arrangement of terminal oxo ligands and with d(Mo═O)$_{av}$ = 1.695 Å and ∠(MoO$_2$)$_{av}$ = 103.2°. The R groups of the 2-CHO and 2-NHCOMe derivatives are directed away from the oxo groups and into a cleft in the Tp$^{i\mathrm{Pr}}$ ligand; these derivatives are characterized by Mo–O–C$_{ipso}$ angles of ca. 131° (conformation 1). The R group(s) in the 2-CO$_2$Me and 2,3-(OMe)$_2$ derivatives lie above the face of the three O-donor atoms (directed away from the Tp$^{i\mathrm{Pr}}$ ligand) and the complexes display Mo–O–C$_{ipso}$ angles of 153.1(2) and 149.7(2)°, respectively (conformation 2). Conformations 1 and 2 are both observed in the positionally disordered 2-COMe and 2-COEt derivatives, the two conformers having Mo–O–C$_{ipso}$ angles of 130–140 and >150°, respectively. The 3-COMe and 3-NEt$_2$ derivatives have substituents that project away from the Tp$^{i\mathrm{Pr}}$ ligand and Mo–O–C$_{ipso}$ angles of 134.2(2) and 147.7(2)°, respectively. Many of the complexes exhibit fluxional behavior on the NMR time scale, consistent with the rapid interconversion of two conformers in solution.

Introduction

Molybdenum enzymes catalyze net oxygen atom transfer reactions involving a wide variety of substrates including carbon monoxide, oxo anions, sulfoxides, *N*-oxides, aldehydes, purines, and pyrimidines.[1−4] They are essential to the health of microorganisms, plants, animals, and humans[1−4] and are vital agents in many of the Earth's biogeochemical cycles.[5,6] In broad terms, the mechanisms of action involve a two-electron substrate redox step that interconverts Mo(VI) and Mo(IV) states.[1−4] In some cases, direct oxygen atom transfer (OAT) is invoked, while in others hydroxylation appears to be the key step. There is strong evidence for hydrogen-bond stabilization and proton-transfer activation of key water-based (oxo, hydroxo, and/or aqua) ligands in many of these enzymes.[1−4] Substrate redox is followed by regeneration of the active site by sequential, one-electron, coupled electron−proton transfer (CEPT) steps, again involving key water-based ligands.[1−4] The combination of OAT and CEPT processes has been achieved in a number of oxo−Mo model systems.[7,8] The effects of hydrogen-bonding[9−11]

* To whom correspondence should be addressed. E-mail: cgyoung@unimelb.edu.au.

(1) Hille, R. *Chem. Rev.* **1996**, *96*, 2757−2816.
(2) Pilato, R. S.; Stiefel, E. I. In *Bioinorganic Catalysis*, 2nd ed.; Reedijk, J., Bouwman, E., Eds.; Marcel Dekker: New York, 1999; pp 81−152.
(3) Tunney, J. M.; McMaster, J.; Garner, C. D. In *Comprehensive Coordination Chemistry II*; McCleverty, J. A., Meyer, T. J., Eds.; Elsevier Pergamon: Amsterdam, 2004; Vol. 8, Chapter 8.18, pp 459−477.
(4) Young, C. G. In *Encyclopedia of Inorganic Chemistry 2*; King, R. B., Ed.; Wiley: Chichester, U.K., 2005; Vol. V, pp 3321−3340.
(5) Stiefel, E. I. In *Metal Ions in Biological Systems*; Sigel, A., Sigel, H., Eds.; Marcel Dekker: New York, 2002; Vol. 39, pp 1−29.
(6) Bertini, I.; Gray, H. B.; Stiefel, E. I.; Valentine, J. S. *Biological Inorganic Chemistry: Structure and Reactivity*; University Science Books: Sausalito, CA, 2007.
(7) Young, C. G. In *Biomimetic Oxidations Catalyzed by Transition Metal Complexes*; Meunier, B., Ed.; Imperial College Press: London, 2000; pp 415−459.
(8) Young, C. G. In *Comprehensive Coordination Chemistry II*; McCleverty, J. A., Meyer, T. J., Eds.; Elsevier Pergamon: Amsterdam, 2004; Vol. 4, Chapter 4.7, pp 415−527.
(9) Ueyama, N.; Okamura, T.; Nakamura, A. *J. Am. Chem. Soc.* **1992**, *114*, 8129−8137.

10.1021/ic701957b CCC: $40.75
Published on Web 01/10/2008

and environment[12] on the chemical and redox behavior of oxo−Mo complexes have also attracted considerable attention.

In molybdoenzyme model systems featuring hydrotris(pyrazolyl)borate ligands, we have demonstrated forward and reverse OAT reactions involving mononuclear *cis*-dioxo−Mo(VI) and oxo−Mo(IV) complexes and CEPT reactions leading to EPR-active oxo(hydroxo)−Mo(V) complexes.[7,13,14] Reactions catalyzing the incorporation of water oxygen into oxidized substrates have also been discovered. The formation of Mo(V) species and the incorporation of water oxygen into substrates are proposed to involve intermediate oxo(aqua)−Mo(IV) or oxo(hydroxo)−Mo(IV/V) complexes.[7,13,14] At the Mo(V) level, *cis*-dioxo−Mo(V) complexes have been isolated and thoroughly characterized but oxo(hydroxo)−Mo(V) species have only been observed in solution or in combination with the conjugate base.[15] Oxo(aqua)−Mo(IV) complexes are rare and few have been isolated and characterized; these invariably adopt a trans geometry, e.g., $[MoO(OH_2)(CN)_4]^{2-}$ and $MoO(OH_2)(dppe)_2$ (dppe = 1,2-bis(diphenylphosphino)ethane).[8]

The isolation of aqua or hydroxo oxo−Mo(IV,V) complexes may be facilitated by building intramolecular H-bonds into the molecular structure. In tris(pyrazolyl)borate complexes, this can, in principle, be achieved by functionalizing the scorpionate ligand or a coligand. Examples of the first strategy include $[CuL(H_2O)]PF_6$ (L = hydrotris{3-(2-pyridyl)pyrazol-1-yl}borate[16] or hydrotris{3-(6-methylpyrid-2-yl)pyrazol-1-yl}borate[17]) where the aqua ligands are H-bonded to pyrazolyl and/or pyridyl nitrogen atoms. Rare earth complexes of the 6-methylpyrid-2-yl ligand also feature aqua ligands stabilized by H-bonds to the pyridyl groups.[18] There are many examples of the second strategy in coordination and organometallic chemistry, due to the propensity of aqua ligands to form H-bonds to coligands, counterions, and/or solvent molecules (especially water). Illustrative examples from the recent literature include carboxylate-stabilized $M(PMe_3)_3(O_2CR)_2(OH_2)H_2$ (M = Mo, W; R = Ph, Bu^t)[19] and methylsquarate-stabilized metal complexes.[20]

Only a few aqua tris(pyrazolyl)borate complexes are known to participate in intramolecular H-bonding. Where the aqua complexes are charged, H-bonding interactions with the counterions are frequently observed. Interactions of this type are present in the solid-state structure of [Tp*WO(OH$_2$)(MeCCMe)](O$_3$SCF$_3$) (Tp* = hydrotris(3,5-dimethylpyrazol-1-yl)borate), reported by Crane et al.;[21] here, the structural unit is dimeric, the aqua ligands of two cationic complexes being H-bonded to two "bridging" triflate anions. Triflate ions also H-bond to the aqua ligands in a range of hydrotris(3-isopropylpyrazol-1-yl)borate (Tp$^{i\mathrm{Pr}}$) complexes of Ru, with the general formulas $[Tp^{i\mathrm{Pr}}Ru(OH_2)_nL_{3-n}](O_3SCF_3)$ (L = neutral ligand).[22]

Chart 1. $^-$OAr-R Ligands, Where Numbers Refer to the Corresponding Tp$^{i\mathrm{Pr}}$MoO$_2$(OAr-R) Complexes

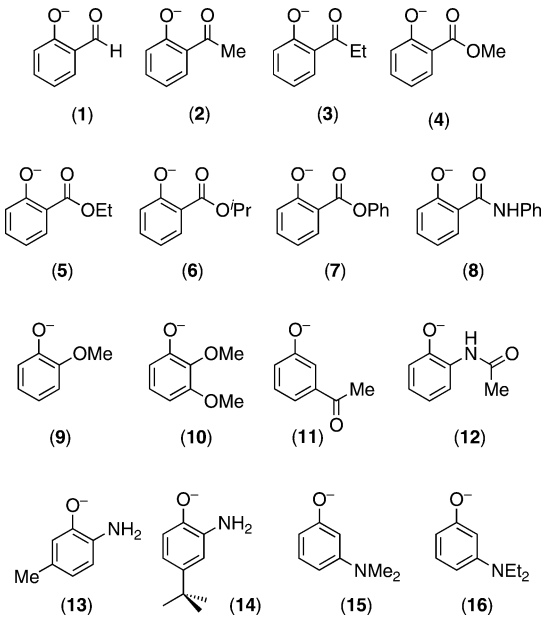

Herein, we report the synthesis and characterization of new dioxo−Mo(VI) complexes, Tp$^{i\mathrm{Pr}}$MoO$_2$(OAr-R), where $^-$OAr-R represents a phenolate derivative containing potential H-bond acceptors/donors (R). The phenolate coligands included in this study and the numbering scheme for their dioxo−Mo(VI) complexes are given in Chart 1. Related *cis*-dioxo−Mo(VI) complexes of Tp$^{i\mathrm{Pr}}$ have been reported for a variety of simple O- and S-donor coligands.[15,23−26] These complexes have served as precursors for novel oxosulfido−Mo(VI),[27] oxo(phosphine oxide)−Mo(IV),[25,28] and carbonyloxo−Mo(IV)[26] complexes. Access to multifunctional com-

(10) Oku, H.; Ueyama, N.; Nakamura, A. *Inorg. Chem.* **1997**, *36*, 1504−1516 and references cited therein.
(11) Conry, R. R.; Tipton, A. A. *J. Biol. Inorg. Chem.* **2001**, *6*, 359−366.
(12) Basu, P.; Nemykin, V. N.; Sengar, R. S. *Inorg. Chem.* **2003**, *42*, 7489−7501.
(13) Xiao, Z.; Bruck, M. A.; Enemark, J. H.; Young, C. G.; Wedd, A. G. *Inorg. Chem.* **1996**, *35*, 7508−7515.
(14) Laughlin, L. J.; Young, C. G. *Inorg. Chem.* **1996**, *35*, 1050−1058.
(15) Xiao, Z.; Gable, R. W.; Wedd, A. G.; Young, C. G. *J. Am. Chem. Soc.* **1996**, *118*, 2912−2921.
(16) Bardwell, D. A.; Jeffery, J. C.; Jones, P. L.; McCleverty, J. A.; Ward, M. D. *J. Chem. Soc., Dalton Trans.* **1995**, 2921−2922.
(17) Humphrey, E. R.; Mann, K. L. V.; Reeves, Z. R.; Behrendt, A.; Jeffery, J. C.; Maher, J. P.; McCleverty, J. A.; Ward, M. D. *New J. Chem.* **1999**, *23*, 417−423.
(18) Reeves, Z. R.; Mann, K. L. V.; Jeffery, J. C.; McCleverty, J. A.; Ward, M. D.; Barigelletti, F.; Armaroli, N. *Dalton Trans.* **1999**, 349−355.
(19) Zhu, G.; Parkin, G. *Inorg. Chem.* **2005**, *44*, 9637−9639.
(20) (a) Alleyne, B. D.; Hosein, H.-A.; Jaggernauth, H.; Hall, L. A.; White, A. J. P.; Williams, D. J. *Inorg. Chem.* **1999**, *38*, 2416−24221. (b) Alleyne, B. D.; Williams, A. R.; Hall, L. A.; White, A. J. P.; Williams, D. J. *Inorg. Chem.* **2001**, *40*, 1045−1051.
(21) Crane, T. W.; White, P. S.; Templeton, J. L. *Inorg. Chem.* **2000**, *39*, 1081−1091.
(22) Takahashi, Y.; Akita, M.; Hikicki, S.; Moro-oka, Y. *Inorg. Chem.* **1998**, *37*, 3186−3194.
(23) Xiao, Z.; Bruck, M. A.; Doyle, C.; Enemark, J. H.; Grittini, C.; Gable, R. W.; Wedd, A. G.; Young, C. G. *Inorg. Chem.* **1995**, *34*, 5950−5962. (Erratum: *Inorg. Chem.* **1996**, *35*, 5752.)
(24) Millar, A. J.; Doonan, C. J.; Laughlin, L. J.; Tiekink, E. R. T.; Young, C. G. *Inorg. Chim. Acta* **2002**, *337*, 393−406.
(25) Doonan, C. J.; Millar, A. J.; Nielsen, D. J.; Young, C. G. *Inorg. Chem.* **2005**, *44*, 4506−4514.
(26) Malarek, M. S.; Evans, D. J.; Smith, P. D.; Bleeker, A. R.; White, J. M.; Young, C. G. *Inorg. Chem.* **2006**, *45*, 2209−2216.
(27) Doonan, C. J.; Nielsen, D. J.; Smith, P. D.; White, J. W.; George, G. N.; Young, C. G. *J. Am. Chem. Soc.* **2006**, *128*, 305−316.
(28) Millar, A. J.; Doonan, C. J.; Smith, P. D.; Nemykin, V. N.; Basu, P.; Young, C. G. *Chem.−Eur. J.* **2005**, *11*, 3255−3267.

plexes lays the groundwork for ongoing investigations aimed at isolating aqua− and hydroxo−Mo(IV,V) complexes relevant to low-valent enzyme states and building extended networks on the basis of H-bonding interactions.

Experimental Section

Materials and Methods. All reactions were performed under an atmosphere of dinitrogen using dried, deoxygenated solvents, but workups were performed in air. Samples of $Tp^{iPr}MoO_2Cl$ were prepared as previously described.[25] Most of the phenols were obtained from Aldrich Chemical Co. and were generally used without purification; discolored samples were purified by sublimation, so as to assist visual assessment of chromatographic separations. The ethyl salicylate and isopropyl salicylate were prepared from salicylic acid and the appropriate alcohol.[29] Column chromatography was performed using silica gel (mesh size 40−200) columns with dimensions of ca. 40−60 cm × ∼2.5 cm diameter.

Infrared spectra were recorded on a Bio-Rad FTS 165 FTIR spectrophotometer as pressed KBr disks. Electrospray ionization mass spectrometric (ESI-MS) experiments were carried out in positive-ion mode using a Micromass Quattro II mass spectrometer using samples dissolved in MeCN or $MeCN/CH_2Cl_2$ or MeCN/MeOH mixtures. 1D NMR spectra were recorded at room temperature on a Varian Unity-Plus 400 MHz spectrometer, while COSY, TOCSY, HMBC, and HMQC spectra were recorded on a stabilized Varian Inova-400 MHz spectrometer. Spectra were referenced to residual solvent peaks (for C_6D_6, δ_H 7.16, δ_C 128.39; for $CDCl_3$, δ_H 7.24, δ_C 77.0); resonances assigned to the Tp^{iPr} ligand are as follows: 5-C*H* (ring), doublets δ 7.7−7.1 (J = 2.4 Hz); 4-C*H* (ring), doublets δ 6.2−5.6 (J = 2.4 Hz); C*H*$(CH_3)_2$, septets δ 4.9−3.2 (J = 6.8 Hz); $CH(CH_3)_2$, doublets δ 1.3−0.7 (J = 6.8 Hz); other resonances are due to the $^-$OAr-R groups (note some peaks were broadened (br) or not observed due to fluxionality). Cyclic voltammograms were recorded using a 2 mm glassy carbon working electrode, platinum counter electrode, and a freshly prepared double-jacketed $Ag/AgNO_3$ reference electrode (10 mM $AgNO_3$ in MeCN with 0.1 M $NBu^n_4PF_6$ and clean silver wire), connected to an Autolab Potentiostat operated by the General Purpose Electrochemical System software (version 4.9). Samples were prepared as 1−2 mM solutions in MeCN with 0.1 M $NBu^n_4PF_6$ as supporting electrolyte and scan rates over the range 10−500 mV s^{-1}. Potentials were referenced against the ferrocene couple, Fc^+/Fc, and are reported relative to SCE. The Fc^+/Fc couple was set to the reported value of +0.400 V vs SCE for acetonitrile/0.1 M $NBu^n_4PF_6$ solutions.[30] Microanalyses were performed by Atlantic Microlab Inc., Norcross, GA.

Syntheses and Characterization. The procedure below was adopted for all the $Tp^{iPr}MoO_2$(OAr-R) complexes; specific conditions or variations are indicated prior to each set of characterization data. Yellow $Tp^{iPr}MoO_2Cl$ (1.00 g; 2 mmol) and the appropriate phenol (5 mmol) were dissolved in CH_2Cl_2 (30 mL) in a Schlenk flask, and then triethylamine (3−4 mL, ca. 20−30 mmol) was added. The reaction mixture was stirred vigorously for 1−7 days and then reduced to low volume (ca. 5 mL) by rotary evaporation. The residue was purified by column chromatography on silica gel using the solvents indicated. The complex usually eluted as the third or fourth band (yellow, orange, or red), after unreacted $Tp^{iPr}MoO_2Cl$, excess parent phenol, and unidentified minor products. The isolated fraction was reduced to dryness and then treated with methanol and refrigerated to yield crystals. The compounds were recrystallized from dichloromethane/hexane or dichloromethane/methanol mixtures.

R = 2-CHO (1): reaction time 1 day; eluent 1:4 CH_2Cl_2/hexane; yield 0.50 g (43%). Anal. Calcd for $C_{25}H_{33}BMoN_6O_4$: C, 51.00; H, 5.65; N, 14.28. Found: C, 50.55; H, 5.76; N, 14.15. IR (KBr, cm^{-1}): ν(BH) 2519 m and 2470 sh,w; ν(C═O) 1687 s; ν(CN) 1506 m; $\nu(MoO_2)$ 934 and 903 s. ^{1}H NMR ($CDCl_3$): δ_H 10.05 (1H, br s), 7.79 (1H, dd, J = 7.6 and 1.6 Hz), 7.67 (1H, d, J = 2.4 Hz), 7.64 (2H, d, J = 2.4 Hz), 7.50 (1H, br m), 7.02 (1H, t, J = 7.6 Hz), 6.85 (1H, br m), 6.17 (1H, d, J = 2.4 Hz), 6.09 (2H, d, J = 2.4 Hz), 4.31 (1H, sept, J = 6.8 Hz), 3.38 (2H, sept, J = 6.8 Hz), 1.30 (6H, d, J = 6.8 Hz), 1.10 (6H, d, J = 6.8 Hz), 0.85 (6H, d, J = 6.8 Hz). $^{13}C\{^1H\}$ NMR ($CDCl_3$): δ_C 190.7, 167.1, 165.3, 164.8, 137.9, 136.5, 136.0, 127.4, 126.3, 121.6, 120.3, 102.8, 102.3, 28.5, 27.6, 24.5, 23.2, 22.8. ESI-MS: m/z 611.5 $[M + Na]^+$, 589.2 $[M + H]^+$, 479.4 $[M - C_6H_9N_2]^+$.

R = 2-COMe (2): reaction time 3 days; eluent CH_2Cl_2; yield 0.50 g (42%). Anal. Calcd for $C_{26}H_{35}BMoN_6O_4$: C, 51.85; H, 5.86; N, 13.95. Found: C, 51.79; H, 5.94; N, 13.93. IR (KBr, cm^{-1}): ν(BH) 2496 and 2460 m; ν(C═O) 1663 s; ν(CN) 1506 s; $\nu(MoO_2)$ 935 and 904 s. ^{1}H NMR (C_6D_6): δ_H 8.17 (1H, br d, J = 7.6 Hz), 7.31 (1H, d, J = 2.4 Hz), 7.14 (2H, d, J = 2.4 Hz), 7.2−6.6 (3H, br m), 5.78 (2H, d, J = 2.4 Hz), 5.62 (1H, d, J = 2.4 Hz), 4.65 (1H, br sept), 3.71 (2H, br sept), ∼2.3 (3H, v br), 1.20 (6H, d, J = 6.8 Hz), 1.11 (6H, d, J = 6.8 Hz), 0.85 (6H, br s). $^{13}C\{^1H\}$ NMR ($CDCl_3$): δ_C 200.3, 166.1 (br) 165.7, 138.9, 136.8, 131.2, 129.5 (br), 122.3 (br), 103.6, 103.2, 29.4, 28.5, 25.8, 24.1, 23.0 (br). ESI-MS: m/z 627.2 $[M + Na]^+$, 605.2 $[M + H]^+$, 495.2 $[M - C_6H_9N_2]^+$.

R = 2-COEt (3): reaction time 3 days; eluent CH_2Cl_2; yield 0.55 g (45%). Anal. Calcd for $C_{27}H_{37}BMoN_6O_4$: C, 52.61; H, 6.05; N, 13.64. Found: C, 52.55; H, 6.05; N, 13.61. IR (KBr, cm^{-1}): ν(BH) 2498 m and 2460 w; ν(C═O) 1668 s; ν(CN) 1506 s; $\nu(MoO_2)$ 934 and 904 s. ^{1}H NMR ($CDCl_3$): δ_H 7.74 (1H, d, J = 8.4 Hz), 7.64 (1H, d, J = 2.4 Hz), 7.62 (2H, d, J = 2.4 Hz), ∼7.1−6.6 (3H, br m), 6.14 (1H, d, J = 2.4 Hz), 6.04 (2H, br d), 4.30 (1H, br), 3.34 (2H, br), ∼2.0 (2H, br m) 1.27 (6H, d, J = 6.8 Hz), 1.07 (6H, d, J = 6.8 Hz), 0.85 (v br), 0.56 (v br). ^{1}H NMR (C_6D_6): δ_H 8.13 (br s), 7.32 (d, J = 2.4 Hz), 7.14 (d, J = 2.4 Hz), 6.71 (br s), 5.79 (d, J = 2.4 Hz), 5.62 (d, J = 2.4 Hz), 4.65 (br s), 3.72 (br s), ∼2.3 (br), 1.19 (d, J = 6.8 Hz), 1.12 (d, J = 6.4 Hz), 0.85 (br s). $^{13}C\{^1H\}$ NMR ($CDCl_3$): δ_C 202.3 (br), 165.0 (br), 164.6, 137.8, 135.6, 134−5 (br), 130.1, 128.5, 121.3, 119−120 (br), 102.4, 102.1, 36−38 (br), 28.3, 27.4, 24.7, 23.0 (2C), 21.8. ESI-MS: m/z 641.2 $[M + Na]^+$, 619.3 $[M + H]^+$, 509.2 $[M - C_6H_9N_2]^+$.

R = 2-CO_2Me (4): reaction time 4 days; eluent CH_2Cl_2; yield 0.40 g (32%). Anal. Calcd for $C_{26}H_{35}BMoN_6O_5$: C, 50.47; H, 5.71; N, 13.59. Found: C, 50.16; H, 5.71; N, 13.47. IR (KBr, cm^{-1}): ν(BH) 2485 and 2458 m; ν(C═O) 1701 s; ν(CN) 1507 s; $\nu(MoO_2)$ 933 and 905 s. ^{1}H NMR ($CDCl_3$): δ_H 7.80 (2H, dd, J = 7.8 and 1.6 Hz), 7.62 (1H, d, J = 2.4 Hz), 7.60 (2H, d, J = 2.4 Hz), 6.90 (2H, br m), 6.15 (1H, d, J = 2.4 Hz), 6.06 (2H, d, J = 2.4 Hz), 4.40 (1H, br sept, J = 6.8 Hz), 3.43 (2H, br sept), 1.29 (6H, d, J = 6.8 Hz), 1.08 (6H, d, J = 6.8 Hz), 0.77 (6H, br s) ($COCH_3$ resonance not observed). $^{13}C\{^1H\}$ NMR ($CDCl_3$): δ_C 167.5, 165.1, 164.8, 137.5, 135.4, 134.0 (br), 131.7, 121.1 (br), 120.1 (br), 102.5, 102.0, 51.7, 28.4, 27.4, 24.8 23.3, 22.2. ESI-MS: m/z 641.3 $[M + Na]^+$, 619.4 $[M + H]^+$, 509.5 $[M - C_6H_9N_2]^+$.

R = 2-CO_2Et (5): reaction time 1 day; eluent 1:1 CH_2Cl_2/hexane; yield 0.41 g (32%). Anal. Calcd for $C_{27}H_{37}BMoN_6O_5$: C, 51.28; H, 5.90; N, 13.29. Found: C, 51.04; H, 6.03; N, 13.33. IR

(29) Vogel, A. I.; Furniss, B. S.; Hannaford, A. J.; Smith, P. W. G.; Tatchell, A. R. *Vogel's Textbook of Practical Organic Chemistry*, 5th ed.; Longman: London, U.K., 1989; Chapter 6.14, pp 1076−1080.

(30) Connelly, N. G.; Gieger, W. E. *Chem. Rev.* **1996**, *96*, 877−910.

(KBr, cm^{-1}): ν(BH) 2489 m and 2459 sh, w; ν(C═O) 1697 s; ν(CN) 1508 s; ν(MoO_2) 933 and 905 s. ^1H NMR ($CDCl_3$): δ_H 7.87 (1H, dd, J = 6.8 and 1.6 Hz), 7.64 (1H, d, J = 2.4 Hz), 7.62 (2H, d, J = 2.4 Hz), 6.90 (2H, br m), 6.15 (1H, d, J = 2.4 Hz), 6.06 (2H, d, J = 2.4 Hz), 4.41 (1H, sept, J = 6.8 Hz), 3.44 (2H, br sept), 1.30 (6H, d, J = 6.8 Hz), 1.10 (6H, d, J = 6.8 Hz), 0.83 (6H, br s) (one Ar-*H* and $COCH_2CH_3$ resonances not observed). $^{13}C\{^1H\}$ NMR ($CDCl_3$): δ_C 167.4, 165.2, 165.0, 137.5, 135.8, 135.5, 132.0 (br), 121.0 (br), 102.6, 102.0, 60.8 (br), 28.4, 27.4, 24.7, 23.3, 22.3. ESI-MS: *m*/*z* 657.3 $[M + Na]^+$, 635.2 $[M + H]^+$, 525.3 $[M - C_6H_9N_2]^+$.

R = 2-CO_2^{i}Pr (6): reaction time 1 day; eluent 1:1 CH_2Cl_2/hexane; yield 0.69 g (54%). Anal. Calcd for $C_{28}H_{39}BMoN_6O_5$: C, 51.99; H, 6.08; N, 13.00. Found: C, 52.17; H, 6.14; N, 13.04. IR (KBr, cm^{-1}): ν(BH) 2489 m and 2459 sh, m; ν(C═O) 1694 s; ν(CN) 1507 s; ν(MoO_2) 933 and 904 s. ^1H NMR ($CDCl_3$): δ_H 7.80 (br), 7.64 (1H, d, J = 2.4 Hz), 7.62 (2H, d, J = 2.4 Hz), 6.90 (br), 6.15 (1H, d, J = 2.4 Hz), 6.06 (2H, d, J = 2.4 Hz), 5.0 (vbr), 4.4 (br), 3.4 (br), 1.29 (3H, d, J = 6.8 Hz), 1.09 (3H, d, J = 6.8 Hz), 0.6−1.0 (br). $^{13}C\{^1H\}$ NMR: spectrum could not be obtained due to decomposition during data acquisition. ESI-MS: *m*/*z* 671.3 $[M + Na]^+$, 649.3 $[M + H]^+$.

R = 2-CO_2Ph (7): reaction time 3 days; eluent 1:1 CH_2Cl_2/hexane; yield 0.35 g (26%). Anal. Calcd for $C_{31}H_{37}BMoN_6O_5$: C, 54.69; H, 5.48; N, 12.35. Found: C, 53.94; H, 5.49; N, 12.20. IR (KBr, cm^{-1}): ν(BH) 2506 m and 2460 sh, w; ν(C═O) 1774 s; ν(CN) 1508 s; ν(MoO_2) 925 and 900 s. ^1H NMR ($CDCl_3$): δ_H 7.95 (1H, dd, J = 7.8 and 2.0 Hz), 7.64 (1H, d, J = 2.4 Hz), 7.5−7.1 (10H, br m), 6.15 (1H, d, J = 2.4 Hz), 5.97 (2H, br d), 4.37 (1H, sept, J = 6.8 Hz), 3.46 (2H, br sept), 1.29 (6H, d, J = 6.8 Hz), 1.10 (6H, d, J = 6.8 Hz), 0.93 (6H, br s). $^{13}C\{^1H\}$ NMR ($CDCl_3$): δ_C 165.6, 165.1, 164.8, 137.6, 135.4, 132.2, 129.0 (br), 125.2 (br), 121.5 (br), 121.2 (br), 120.7 (br), 102.5, 102.1, 28.4, 27.5, 24.8, 23.3, 22.3. ESI-MS: *m*/*z* 603.6 $[M + Na]^+$, 681.2 $[M + H]^+$, 571.6 $[M - C_6H_9N_2]^+$.

R = 2-CONHPh (8): reaction time 1 day; eluent CH_2Cl_2; yield 0.87 g (64%). Anal. Calcd for $C_{31}H_{38}BMoN_7O_4$: C, 54.80; H, 5.64; N, 14.43. Found: C, 54.09; H, 5.71; N, 14.17. IR (KBr, cm^{-1}): ν(NH) 3315 s; ν(BH) 2521 sh, w and 2484 m; ν(C═O) 1659 s; ν(CN) 1504 s; ν(MoO_2) 935 and 904 s. ^1H NMR ($CDCl_3$): δ_H 9.93 (1H, br s), 8.33 (1H, d, J = 8.0 Hz), 7.74 (1H, d, J = 2.4 Hz), 7.64 (3H, br m), 7.50 (1H, d, J = 8.0 Hz), 7.19 (1H, t, J = 7.8 Hz), 6.96 (2H, t, J = 7.6 Hz), 6.88 (1H, d, J = 7.6 Hz), 6.33 (2H, d, J = 7.6 Hz), 6.22 (1H, d, J = 2.4 Hz), 5.98 (2H, d, J = 2.4 Hz), 4.25 (1H, sept, J = 6.8 Hz), 3.26 (2H, sept, J = 6.8 Hz), 1.31 (6H, d, J = 6.8 Hz), 1.07 (6H, d, J = 6.8 Hz), 0.91 (6H, d, J = 6.8 Hz). $^{13}C\{^1H\}$ NMR ($CDCl_3$): δ_C 165.7, 163.2, 162.7, 138.3, 138.2, 136.3, 134.2, 131.7, 128.4, 123.3, 122.3, 122.1, 121.0, 119.2, 103.1, 103.0, 28.6, 27.6, 24.7, 23.2, 22.3. ESI-MS: *m*/*z* 682.2 $[M + H]^+$, 572.4 $[M - C_6H_9N_2]^+$.

R = 2-OMe (9): reaction time 3 days; eluent CH_2Cl_2; yield 0.95 g (80%). Anal. Calcd for $C_{25}H_{35}BMoN_6O_4$: C, 50.80; H, 5.98; N, 14.24. Found: C, 50.71; H, 6.02; N, 14.12. IR (KBr, cm^{-1}): ν(BH) 2520 m and 2466 w; ν(CN) 1507 s; ν(MoO_2) 926 and 901 s. ^1H NMR ($CDCl_3$): δ_H 7.58 (1H, d, J = 2.4 Hz), 7.56 (1H, d, J = 2.4 Hz), 6.85−6.74 (2H, m), 6.70 (1H, dt, J = 8.0 and 2.0 Hz), 6.47 (1H, d, J = 7.6 Hz), 6.09 (1H, d, J = 2.4 Hz), 6.01 (2H, d, J = 2.4 Hz), 4.4 (1H, sept, J = 6.8 Hz), 3.65 (3H, s), 3.43 (2H, sept, J = 6.8 Hz), 1.24 (6H, d, J = 6.8 Hz), 1.06 (6H, d, J = 6.8 Hz), 0.82 (6H, d, J = 6.8 Hz). $^{13}C\{^1H\}$ NMR ($CDCl_3$): δ_C 165.9, 165.7, 154.2, 151.1, 138.0, 136.4, 122.7, 122.0, 120.4, 113.1, 103.3, 102.7, 56.7, 29.3, 28.3, 25.3, 24.3, 23.4. ESI-MS: *m*/*z* 593.6 $[M + H]^+$, 483.5 $[M - C_6H_9N_2]^+$.

R = 2,3-$(OMe)_2$ (10): reaction time 3 days; eluent CH_2Cl_2; yield 1.10 g (90%). Anal. Calcd for $C_{26}H_{37}BMoN_6O_5$: C, 50.34; H, 6.01; N, 13.55. Found: C, 49.79; H, 5.85; N, 13.16. IR (KBr, cm^{-1}): ν(BH) 2503 m and 2466 w; ν(CN) 1507 s; ν(MoO_2) 925 and 903 s. ^1H NMR (C_6D_6): δ_H 7.36 (2H, d, J = 2.4 Hz), 7.19 (1H, d, J = 2.4 Hz), 6.61 (1H, t, J = 8.2 Hz), 6.28 and 6.24 (each 1H, dd, J = 8.2 and 1.6 Hz), 5.87 (2H, d, J = 2.4 Hz), 5.66 (1H, d, J = 2.4 Hz), 4.83 (1H, sept, J = 6.8 Hz), 3.98 (2H, sept, J = 6.8 Hz), 3.78 (3H, s), 3.33 (3H, s), 1.23 (6H, d, J = 6.8 Hz), 1.20 (6H, d, J = 6.8 Hz), 1.00 (6H, d, J = 6.8 Hz). $^{13}C\{^1H\}$ NMR (C_6D_6): δ_C 165.7, 165.7, 158.1, 154.8, 140.9, 137.6, 135.9, 123.4, 113.4, 107.0, 103.1, 102.7, 61.1, 56.1, 29.0, 28.2, 25.2, 23.6, 23.0. See Supporting Information for complete assignments of ^1H and ^{13}C NMR spectra. ESI-MS: *m*/*z* 645.2 $[M + Na]^+$, 623.2 $[M + H]^+$, 513.2 $[M - C_6H_9N_2]^+$.

R = 3-COMe (11): reaction time 3 days; eluent CH_2Cl_2; yield 0.55 g (46%). Anal. Calcd for $C_{26}H_{35}BMoN_6O_4$: C, 51.85; H, 5.86; N, 13.95. Found: C, 51.50; H, 5.91; N, 13.79. IR (KBr, cm^{-1}): ν(BH) 2486 and 2460 m; ν(C═O) 1683 s; ν(CN) 1507 s; ν(MoO_2) 931s and 900 s. ^1H NMR ($CDCl_3$): δ_H 7.62 (1H, br d), 7.60 (2H, br d), 7.48 (1H, d, J = 7.2 Hz), 7.28 (1H, t, J = 7.2 Hz), 6.99 (1H, m), 6.12 (1H, br d), 6.04 (2H, br d), 4.32 (1H, sept, J = 6.8 Hz), 3.42 (2H, sept, J = 6.8 Hz), 2.39 (3H, s), 1.25 (6H, d, J = 6.8 Hz), 1.07 (6H, d, J = 6.8 Hz), 0.81 (6H, d, J = 6.8 Hz). $^{13}C\{^1H\}$ NMR ($CDCl_3$): δ_C (CO resonance not observed): 166.2, 165.6, 164.5, 139.2, 138.5, 136.6, 130.5, 124.7, 121.9, 119.8, 103.5, 103.0, 29.3, 28.4, 27.8, 25.2, 24.2, 23.8. ESI-MS: *m*/*z* 605.2 $[M + H]^+$.

R = 2-NHCOMe (12): reaction time 5 days; eluent 9:1 CH_2Cl_2/ethyl acetate; yield 0.49 g (40%). Anal. Calcd for $C_{26}H_{36}BMoN_7O_4$: C, 50.58; H, 5.88; N, 15.88. Found: C, 50.66; H, 5.90; N, 15.89. IR (KBr, cm^{-1}): ν(NH) 3401 s; ν(BH) 2498 m, 2462 m; ν(C═O) 1690 s; ν(CN) 1506 s; ν(MoO_2) 935 and 903 s. ^1H NMR ($CDCl_3$): δ_H 8.21 (1H, apparent d), 7.62 (3H, overlapping d), 7.3−6.9 (4H, br m), 6.13 (1H, d, J = 2.4 Hz), 6.09 (2H, br d), 4.27 (1H, sept, J = 6.8 Hz), 3.31 (2H, sept, J = 6.8 Hz); 1.25 (6H, d, J = 6.8 Hz), 1.05 (6H, d, J = 6.8 Hz), 0.81 (6H, br s). $^{13}C\{^1H\}$ NMR ($CDCl_3$): δ_C 165.2, 165.1, 137.7, 135.8, 124.0 (br), 122.3 (br), 119.2 (br), 117.0, 102.6, 102.5, 102.3, 28.3, 27.4, 24.6, 23.0, 22.2 (br). ESI-MS: *m*/ *z* 642.2 $[M + Na]^+$, 620.3 $[M + H]^+$, 510.2 $[M - C_6H_9N_2]^+$.

R = 2-NH_2-5-Me (13): reaction time 5 days; eluent CH_2Cl_2; yield <150 mg (<13%). Anal. Calcd for $C_{25}H_{36}BMoN_7O_3$: C, 50.95; H, 6.16; N, 16.64. Found: C, 50.70; H, 6.19; N, 16.74. IR (KBr, cm^{-1}): ν(NH) 3427 m; ν(BH) 2502 m; ν(CN) 1506 s; ν(MoO_2) 933 and 902 s. ^1H NMR (C_6D_6): δ_H 7.38 (2H, d, J = 2.4 Hz), 7.22 (1H, d, J = 2.4 Hz), 6.60 (1H, dd, J = 7.6 and 2.0 Hz), 6.36 (1H, d, J = 7.6 Hz), 5.90 (2H, d, J = 2.4 Hz), 5.67 (1H, d, J = 2.4 Hz), 4.81 (1H, sept, J = 6.8 Hz), 3.84 (2H, sept, J = 6.8 Hz), 2.07 (3H, s), 1.22 (6H, d, J = 6.8 Hz), 1.15 (6H, d, J = 6.8 Hz), 1.09 (6H, d, J = 6.8 Hz). $^{13}C\{^1H\}$ NMR (C_6D_6): δ_C 165.9, 165.8, 152.9, 137.6, 136.0 (2C), 135.4, 123.8, 120.2, 115.1, 103.1, 102.7, 29.0, 28.2, 25.0, 23.6, 23.3, 21.1. ESI-MS: *m*/*z* 614.2 $[M + Na]^+$, 592.2 $[M + H]^+$, 482.2 $[M - C_6H_9N_2]^+$.

R = 2-NH_2-4-Bu^t (14): reaction time 5 days; eluent CH_2Cl_2; yield <150 mg (<12%). Anal. Calcd for $C_{28}H_{43}BMoN_7O_3$: C, 53.26; H, 6.70; N, 15.53. Found: C, 53.37; H, 6.79; N, 15.57. IR (KBr, cm^{-1}): ν(NH) 3479 m and 3382 s; ν(BH) 2493 m, 2459 m; ν(CN) 1505 s; ν(MoO_2) 921 br, s and 899 s. ^1H NMR (C_6D_6): δ_H 7.38 (2H, d, J = 2.4 Hz), 7.21 (1H, d, J = 2.4 Hz), 6.66 (1H, apparent dd, J = 7.6 and 2.0 Hz), 6.51 (1H, d, J = 2.0 Hz), 5.90 (2H, d, J = 2.4 Hz), 5.67 (1H, d, J = 2.4 Hz), 4.82 (1H, sept, J = 6.8 Hz), 3.84 (2H, sept, J = 6.8 Hz), 3.09 (2H, br s), 1.23 (6H, d, J = 6.8 Hz), 1.20 (9H, s), 1.14 (6H, d, J = 6.8 Hz), 1.04 (6H, d,

Table 1. Crystallographic Data

param	1	2	3	4	11	12	16
formula	$C_{25}H_{33}BMoN_6O_4$	$C_{26}H_{35}BMoN_6O_4$	$C_{27}H_{37}BMoN_6O_4$	$C_{26}H_{35}BMoN_6O_5$	$C_{26}H_{35}BMoN_6O_4$	$C_{26}H_{36}BM\ oN_7O_4$	$C_{28}H_{42}BMoN_7O_3$
formula mass	588.32	602.35	616.38	618.35	602.35	617.37	631.44
cryst system	monoclinic	orthorhombic	orthorhombic	orthorhombic	monoclinic	orthorhombic	monoclinic
space group	$P2_1/c$	*Pbca*	*Pbca*	*Pbca*	$P2_1/n$	*Pbca*	$P2_1/n$
a, Å	14.955(3)	10.8523(6)	10.8083(5)	10.9987(14)	13.022(5)	10.6447(6)	10.2236(8)
b, Å	10.4211(18)	18.1850(10)	18.5871(9)	17.4697(22)	13.115(5)	18.8261(11)	22.0927(16)
c, Å	18.780(3)	29.4125(16)	29.9129(15)	29.6741(36)	16.491(5)	30.8637(18)	14.1767(11)
β, deg	108.256(3)	90	90	90	105.425(5)	90	103.3980(10)
V, Å^3	2779.5(8)	5804.5(6)	6009.4(5)	5701.7(12)	2714.9(17)	6185.0(6)	3114.9(4)
Z	4	8	8	8	4	8	4
T, K	130	293	293	130	130	293	293
ρ, g cm^{-3}	1.406	1.379	1.363	1.441	1.474	1.326	1.346
μ, cm^{-1}	5.13	4.93	4.78	5.06	4.78	4.65	4.61
data	16 489	34 527	35 724	33 712	13 136	36 749	19 397
unique data	6289	6650	6862	6734	6166	7087	7076
R_1 [$I > 2\sigma(I)$][a]	0.0280	0.0639	0.0506	0.0442	0.0395	0.0605	0.0463
wR_2 (F^2, all data)[b]	0.0753	0.1251	0.1128	0.1070	0.0716	0.1216	0.1055
GOF	1.032	1.226	1.160	1.077	0.917	1.110	1.130

[a] $R_1 = \Sigma||F_o| - |F_c||/\Sigma|F_o|$. [b] $wR_2 = \{[\Sigma w(F_o^2 - F_c^2)^2/\Sigma(w|F_o^2|)^2]\}^{1/2}$.

$J = 6.8$ Hz). $^{13}C\{^1H\}$ NMR (C_6D_6): δ_C 165.9, 165.8, 150.7, 145.9, 137.6, 137.2, 136.0, 118.7, 116.0, 112.5, 103.1, 102.7, 34.6, 32.0, 29.0, 28.1, 25.0, 23.6, 23.3. ESI-MS: *m*/*z* 656.2 $[M + Na]^+$, 634.3 $[M + H]^+$, 524.2 $[M - C_6H_9N_2]^+$.

R = 3-NMe$_2$ (15): reaction time 3 days; eluent 3:2 CH_2Cl_2/hexane; yield 0.54 g (45%). Anal. Calcd for $C_{26}H_{38}BMoN_7O_3$: C, 51.76, H, 6.35, N, 16.25. Found: C, 51.71, H, 6.30, N, 16.19. IR (KBr, cm^{-1}): ν(BH) 2575 br, w and 2496 w; ν(CN) 1506 s; ν(MoO_2) 924 and 903 s. ^1H NMR ($CDCl_3$): δ_H 7.60 (1H, d, J = 2.4 Hz), 7.58 (2H, d, J = 2.4 Hz), 7.10 (1H, t, J = 7.6), 6.34 (2H, br), 6.12 (1H, d, J = 2.4 Hz), 6.05 (2H, d, J = 2.4), 6.00 (1H, br s), 4.37 (1H, sept, J = 6.8 Hz), 3.50 (2H, sept, J = 6.8 Hz), 2.80 (6H, s), 1.26 (6H, d, J = 6.8 Hz), 1.09 (6H, d, J = 6.8 Hz), 0.90 (6H, d, J = 6.8 Hz). $^{13}C\{^1H\}$ NMR ($CDCl_3$): δ_C 164.9, 164.7, 164.6, 151.5, 137.0, 135.3, 129.3, 103.5, 102.3, 101.7, 40.8, 28.2, 27.2, 24.1, 23.2, 22.9 (Ar-4/Ar-6 undetected). See Supporting Information for complete assignments of ^1H and ^{13}C NMR spectra. ESI-MS: *m*/*z* 628.1 $[M + Na]^+$, 606.2 $[M + H]^+$, 496.2 $[M - C_6H_9N_2]^+$.

R = 3-NEt$_2$ (16): reaction time 3 days; eluent 3:2 CH_2Cl_2/hexane; yield 0.57 g (45%). Anal. Calcd for $C_{28}H_{42}BMoN_7O_3$: C, 53.26; H, 6.70; N, 15.53. Found: C, 52.96; H, 6.73; N, 15.54. IR (KBr, cm^{-1}): ν(BH) 2544 br, w; ν(CN) 1506 s; ν(MoO_2) 920 and 898 s. ^1H NMR ($CDCl_3$): δ_H 7.59 (1H, d, J = 2.4 Hz), 7.57 (2H, d, J = 2.4 Hz), 7.04 (1H, t, J = 8.0 Hz), 6.26 and 6.20 (each 1H, dd, J = 7.2 and 2.2 Hz), 6.11 (1H, d, J = 2.4 Hz), 6.04 (2H, d, J = 2.4 Hz), 5.95 (t, 1H, J = 2.4 Hz), 4.40 (1H, sept, J = 6.8 Hz), 3.53 (2H, sept, J = 6.8 Hz), 3.19 (4H, q, J = 7.2 Hz), 1.26 (6H, d, J = 6.8 Hz), 1.09 (6H, d, J = 6.8 Hz), 1.02 (6H, t, J = 7.2 Hz), 0.93 (6H, d, J = 6.8 Hz). $^{13}C\{^1H\}$ NMR ($CDCl_3$): δ_C 164.9, 164.6, 148.8, 136.9, 135.3, 129.5, 106.4, 106.0, 102.6, 102.2, 101.7, 44.3, 28.2, 27.2, 24.1, 23.2, 22.9, 12.5. See Supporting Information for complete assignments of ^1H and ^{13}C NMR spectra. ESI-MS: *m*/*z* 656.2 $[M + Na]^+$, 634.2 $[M + H]^+$, 524.2 $[M - C_6H_9N_2]^+$.

X-ray Crystallography. Crystals were grown by slow diffusion of methanol into dichloromethane solutions of freshly chromatographed samples of the complexes. The exceptions were **16**, where hexane was substituted for methanol, and **12**, where crystals were obtained from slow evaporation of an ethyl acetate solution of the complex. Crystal data are provided in Table 1.

Diffraction data were collected using a Bruker CCD diffractometer with a sealed tube Mo Kα (0.710 73 Å) radiation source. Structures were solved using direct methods and refined with SHELX-97[31] with the exception of the structure of **16**, which required the application of SHELX-86.[32] A preliminary structure is also available for **10** (see Supporting Information).

All 7 structures have a single molecule occupying the asymmetric unit, and each was refined using anisotropic thermal parameters for all non-hydrogen atoms. All hydrogen atoms were geometrically fixed using the riding model. For **2** and **3**, the phenolic coligands displayed positional disorder over two sites and were modeled for a total occupancy of one. For **16**, one of the Et groups was modeled over two positions. Molecular diagrams were generated using ORTEP 3.[33] Selected distances and angles are presented in Table 2.

Results and Discussion

Synthesis and Characterization. Red/orange *cis*-Tp^{iPr}-MoO_2(OAr-R) were synthesized by metathesis according to eq 1. Optimized syntheses are reported; longer reaction times or gentle heating only resulted in decomposition. The air-stable complexes were purified by column chromatography and recrystallization from dichloromethane/hexane or dichloromethane/methanol mixtures.

$$Tp^{iPr}MoO_2Cl + HOAr\text{-}R + NEt_3 \rightarrow Tp^{iPr}MoO_2(OAr\text{-}R) + NEt_3HCl \quad (1)$$

The Tp^{iPr}MoO_2(OAr-R) complexes are generally stable for weeks in solution (CH_2Cl_2/MeOH) in the presence of the parent phenol but are unstable in its absence; consequently, incomplete chromatographic separation of these complexes from their parent phenols actually facilitates the isolation of pure samples upon final recrystallization. Degradation leads to the formation of di-, tetra-, octa-, and/or hexadecanuclear[34] species, depending on the phenolate derivative and conditions. Correct microanalyses were obtained for all title complexes. Positive-ion ESI-MS revealed molecular ions [M

(31) Sheldrick, G. M. *SHELXL-97 Program for Crystal Structure Refinement*; University of Göttingen: Göttingen, Germany, 1997.
(32) Sheldrick, G. M. *Acta Crystallogr.* **1990**, *A46*, 467.
(33) Farrugia, L. J. *J. Appl. Crystallogr.* **1997**, *30*, 565.
(34) Hill, L. M. R.; Abrahams, B. F.; Young, C. G. *Chem.−Eur. J.* **2008**, in press.

Table 2. Selected Bond Distances (Å) and Angles (deg)

param	**1**	**2**[a]	**3**[a]	**4**	**11**	**12**	**16**
Mo1−O1	1.9407(12)	1.923(2)	1.927(2)	1.903(2)	1.9081(19)	1.939(2)	1.8950(18)
Mo1−O2	1.7042(13)	1.690(3)	1.691(2)	1.6994(19)	1.6940(18)	1.690(2)	1.697(2)
Mo1−O3	1.6956(13)	1.690(3)	1.688(2)	1.698(2)	1.6898(18)	1.687(2)	1.6978(19)
Mo1−N11	2.1856(14)	2.191(3)	2.188(2)	2.184(2)	2.213(2)	2.189(2)	2.204(2)
Mo1−N21	2.3185(16)	2.337(3)	2.314(3)	2.334(2)	2.306(2)	2.329(3)	2.320(2)
Mo1−N31	2.3133(15)	2.314(3)	2.322(3)	2.325(2)	2.290(2)	2.320(3)	2.338(2)
Mo1−O1−C1	131.62(11)	138.6(3), 161.8(6)	131.0(3), 151.5(4)	153.1(2)	134.2(2)	131.1(2)	147.71(17)
O2−Mo1−O3	102.89(7)	103.03(16)	102.84(12)	103.88(10)	103.04(9)	102.77(12)	103.61(10)
O1−Mo1−O2	100.57(6)	100.32(13)	100.52(10)	100.15(9)	101.93(8)	100.42(10)	103.01(9)
O1−Mo1−O3	100.86(6)	101.32(12)	100.29(10)	102.21(10)	100.85(8)	100.38(10)	100.98(9)
N11−Mo1−O1	159.14(5)	158.44(12)	160.95(9)	160.08(9)	161.90(8)	159.27(10)	159.20(8)
N11−Mo1−O2	92.98(6)	92.93(12)	91.03(10)	91.23(9)	90.74(8)	92.75(10)	90.57(9)
N11−Mo1−O3	91.38(6)	92.06(13)	91.73(10)	90.71(10)	88.61(8)	92.13(11)	90.83(9)
N21−Mo1−O1	83.78(5)	84.09(11)	85.73(9)	85.93(9)	85.29(8)	83.83(11)	84.98(8)
N21−Mo1−O2	166.53(6)	167.68(13)	164.86(11)	165.56(9)	163.32(8)	166.88(13)	163.73(10)
N21−Mo1−O3	88.64(6)	87.25(12)	89.43(11)	87.41(9)	90.13(8)	88.52(12)	88.47(9)
N31−Mo1−O1	83.84(5)	84.01(11)	85.43(9)	85.22(9)	86.64(8)	83.82(11)	85.66(8)
N31−Mo1−O2	89.33(6)	89.50(13)	87.71(10)	88.84(10)	88.33(8)	89.86(13)	86.57(9)
N31−Mo1−O3	165.72(6)	165.15(12)	166.73(11)	163.68(10)	164.61(8)	165.60(13)	166.07(9)
Mo1−(O_3)[b]	0.7936(8)	0.7860(16)	0.7935(13)	0.7741(16)	0.7761(12)	0.7950(15)	0.7628(12)
Mo1−(N_3)[c]	1.5293(9)	1.5369(18)	1.5316(15)	1.5470(18)	1.5375(15)	1.5343(15)	1.5476(13)
Mo1−equatorial[d]	0.1086(7)	0.1131(14)	0.1282(12)	0.145(2)	0.154(1)	0.1206(14)	0.1555(11)
Ph/(Mo1,N11,B)[e]	3.0(1)	16.2(6), 19(1)	6.0(5), 11.3(6)	25.1(2)	23.1(2)	4.6(3)	42.1(2)
Mo1−O1−C1−C2[f]	177.55(12)	168(2), 131(4)	177.2(5), 168(2)	129.6(5)	20.2(4)	176.7(3)	137.0(3)

[a] Parameters for the major positional form, except where two values are given (the first pertaining to the major positional form, the second to the minor form). [b] The displacement of the Mo1 atom and the O1,O2,O3 plane (Å). [c] The displacement of the Mo atom from the N11,N21,N31 plane (Å). [d] The displacement of the Mo atom from the equatorial (O2,O3,N21,N31) plane (Å). [e] Dihedral angle between the plane of the phenolate ring (C_1−C_6) and the Mo1,N11,B plane (deg). [f] Torsion angle (deg) (both positive and negative angles are represented in the lattices).

+ H]$^+$, along with [M + Na]$^+$ and [M −$C_6H_9N_2$]$^+$ (corresponding to the loss of a 3-isopropylpyrazolate unit).

Infrared spectra exhibited bands at ca. 935 and 900 cm^{-1}, which were assigned to the ν_s(MoO_2) and ν_{as}(MoO_2) modes of the *cis*-dioxo−Mo(VI) moiety, respectively; the positions and intensities of these bands were consistent with literature values for related complexes.[8,25] Bands characteristic of the Tp^{iPr} (ν(BH) 2575−2458 cm^{-1}, ν(CN) ca. 1507 cm^{-1}) and phenolate (ca. 1570 cm^{-1} and 1260 cm^{-1}) ligands were also present.[35] The substitution patterns of the 2-R- and 3-R-phenolate coligands are well-represented in the fingerprint region (900−680 cm^{-1}), with CH out-of-plane bends corresponding to the patterns of substitution.[36] The primary amine and amide groups gave rise to characteristic N−H stretching bands around 3380−3480 and 3315−3400 cm^{-1}, respectively.[35] All such bands, except the ν(NH) band of **13**, were reasonably strong. The carbonyl groups exhibit bands from 1659−1774 cm^{-1} that are assigned to the carbonyl stretching mode.

^{1}H NMR spectra of the Tp^{iPr}MoO_2(OAr-R) complexes revealed effective C_s symmetry in solution, with a 2:1 intensity ratio for the various sets of pyrazole ring and isopropyl methine resonances and a 1:1:1 intensity ratio for the three sets of inequivalent isopropyl methyl groups. Complexes **2**−**6** and **12** exhibited highly fluxional behavior leading to broad or absent signals at room temperature, consistent with the interconversion of the conformers identified by X-ray crystallography (vide infra). Fluxional behavior and long relaxation times meant that the phenolate carbon atoms of some derivatives were not detectable by ^{13}C NMR spectroscopy (only major resonances are reported). Two-dimensional NMR techniques permitted detailed ^{1}H and ^{13}C NMR assignments for a number of nonfluxional derivatives (see Supporting Information).

Table 3. $E_{1/2}$ (V vs SCE) Values for the Series Tp^{iPr}MoO_2(OAr-R)

R	$E_{1/2}$ (V)	ΔE_{pp} (mV)	I_{pa}/I_{pc}
2-CO_2Ph (**7**)	−0.924[a]		
3-NMe_2 (**15**)	−0.836	95	1.02
3-NEt_2 (**16**)	−0.833	85	0.92
2-NH_2-4-Bu^t (**14**)	−0.815	87	0.97
2-OMe (**9**)	−0.805	82	0.96
2-NH_2-5-Me (**13**)	−0.804	82	0.96
2,3-$(OMe)_2$ (**10**)	−0.785	84	0.95
none[b]	−0.782	93	0.97
2-CO_2^{i}Pr (**6**)	−0.781	94	1.00
2-CO_2Et (**5**)	−0.775	99	1.01
2-CO_2Me (**4**)	−0.757	103	1.01
3-COMe (**11**)	−0.725	95	0.99
2-COEt (**3**)	−0.711	87	0.98
2-COMe (**2**)	−0.700	105	1.02
2-NHCOMe (**12**)	−0.677	87	0.96
2-CHO (**1**)	−0.638	83	0.96
CONHPh (**8**)	−0.598	84	0.96

[a] Irreversible. [b] Tp^{iPr}MoO_2(OPh); $E_{1/2}$ recorded here is close to the reported $E_{1/2}$ of −0.780 V vs SCE.[23]

Electrochemistry. The electrochemical properties of the dioxo−Mo(VI) complexes in acetonitrile were investigated by cyclic voltammetry; the results of these studies are summarized in Table 3. All complexes, except **7**, exhibited a single, reversible, one-electron reduction in the potential range −0.836 to −0.598 V vs SCE; complex **7** exhibited an irreversible reduction at −0.924 V vs SCE. A representative cyclic voltammogram is shown in Figure 1. No other electrochemical processes were observed. Consistent with

(35) Silverstein, R. M.; Bassler, C. G.; Morrill, T. C. *Spectrophotometric Identification of Organic Compounds*, 4th ed.; Wiley: New York, 1981.
(36) Williams, D. H.; Fleming, I. *Spectroscopic Methods in Organic Chemistry*, 5th ed.; McGraw-Hill: London, 1995.

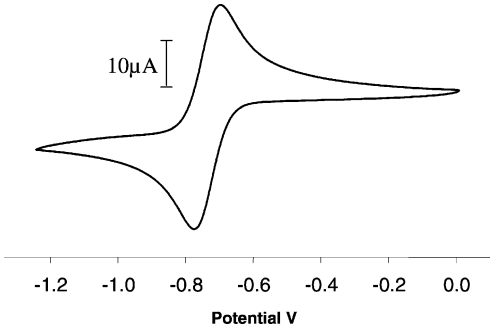

Figure 1. Cyclic voltammogram of **11** at 100 mV s^{-1}, in 0.1 mM solution in MeCN and 0.1 M $NBu^n_4PF_6$ (potential vs SCE).

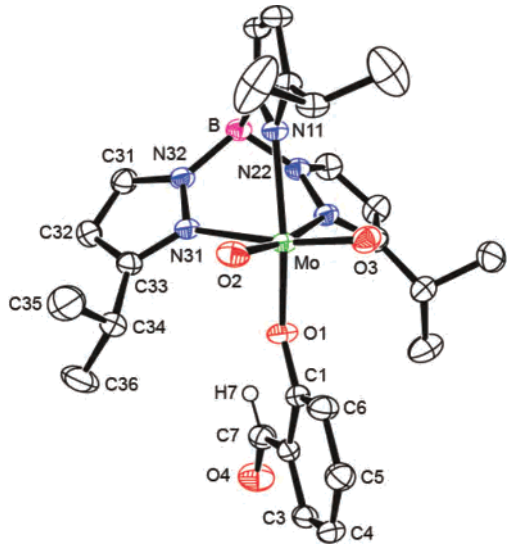

Figure 2. ORTEP projection of **1** drawn at 40% probability. The labeling of the pyrazole groups containing N11 and N22 follows that shown for the group containing N31.

diffusion-controlled redox processes,[37] the $E_{1/2}$ values were independent of scan rates, peak current ratios were close to unity, and plots of current vs $\nu^{1/2}$ (where ν is the scan rate) were strictly linear. Electron-donating substituents shifted the reduction potentials to more negative values; electron-withdrawing substituents shifted potentials to more positive values. The latter trend reflects the effective increase in the nuclear charge at the metal center with electron-withdrawing coligand substituents, resulting in a lowered energy of the LUMO and consequently a more favorable metal-centered reduction.[23−25] The reversible electrochemical reductions are indicative of reduction to stable Mo(V) anions under the conditions of the experiments and are consistent with previous studies of related tris(pyrazolyl)borate complexes.[23−25]

Crystal Structures. The X-ray crystal structures of seven complexes were determined and representative structures are shown in Figures 2−6. ORTEP projections of the other structures, along with details of the preliminary structure of **10**, are provided in the Supporting Information.

The complexes display distorted octahedral geometries defined by mutually cis oxo and phenolate ligands and a tridentate *fac*-Tp^{iPr} ligand. The isopropyl substituents of the

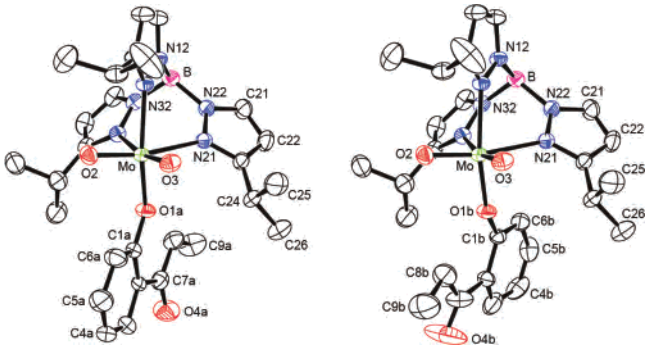

Figure 3. ORTEP projections of the two positional forms of **3** drawn at the 30% probability level: left, 61% occupancy; right, 39% occupancy. The labeling of the pyrazole groups containing N12 and N32 follows that shown for the group containing N21.

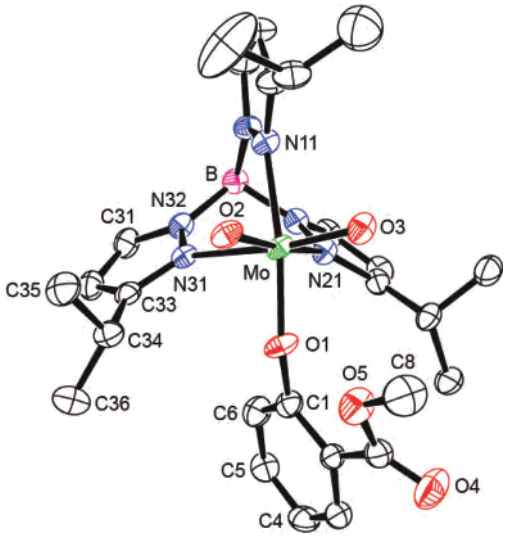

Figure 4. ORTEP projection of **4** drawn at the 40% probability level. The labeling of the pyrazole groups containing N11 and N21 follows that shown for the group containing N31.

Tp^{iPr} ligand adopt the same conformation in all structures, the methine hydrogen atoms pointing toward the pseudo-3-fold axis of the Mo Tp^{iPr} unit. In **2**, the ^{i}Pr group on the pyrazole trans to the phenolate is rotated ca. 20° from its idealized position straddling the pseudo-mirror plane of the pyrazole−Mo unit. In **3**, one of the two positions for the disordered ^{i}Pr groups trans to the phenolate adopts a similar conformation, the second adopting the idealized conformation. Packing forces are thought to be responsible for these minor perturbations to idealized structures. The structures differ in the arrangement of the phenolate coligands and the nature of the solid state interactions observed (vide infra).

The Mo═O distances range from 1.687(2)−1.7042(13) Å and are within the observed range of 1.62−1.72 Å for dioxomolybdenum(VI) complexes[8,38,39] and similar to previously reported distances of 1.696−1.705 Å for scorpionate complexes of Mo(VI).[15,23−26] The O2−Mo1−O3 angles range from 102.77(12) to 103.88(10)°, in line with values

(37) Christensen, P. A.; Hamnett, A. *Techniques and Mechanisms in Electrochemistry*; Chapman and Hall: Oxford, U.K., 1994.

(38) Orpen, A. G.; Brammer, L.; Allen, F. H.; Kennard, O.; Watson, D. G.; Taylor, R. *J. Chem. Soc., Dalton Trans.* **1989**, S1−S83.

(39) Stiefel, E. I. In *Comprehensive Coordination Chemistry*; Wilkinson, G., Gillard, R. D., McCleverty, J. A., Eds.; Pergamon: Oxford, U.K., 1987; Chapter 36.5, pp 1375−1420.

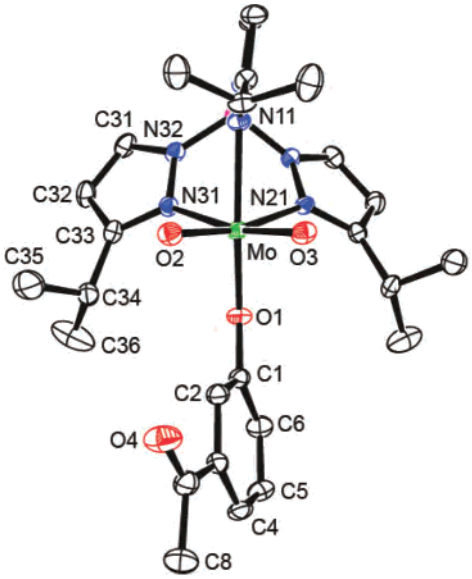

Figure 5. ORTEP projection of **11** drawn at the 40% probability level. The labeling of the pyrazole groups containing N11 and N21 follows that shown for the group containing N31.

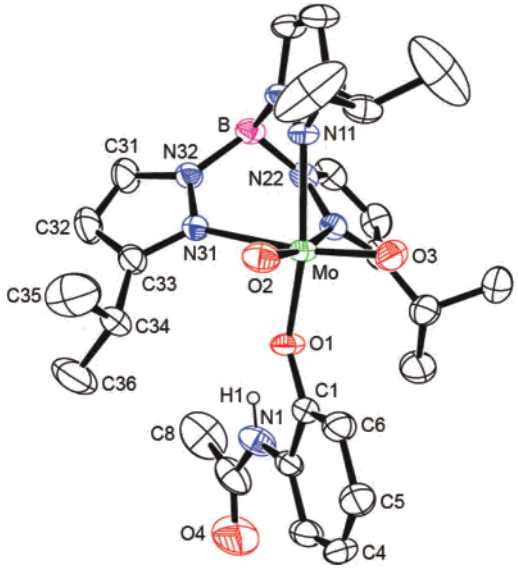

Figure 6. ORTEP projection of **12** drawn at the 30% probability level. The labeling of the pyrazole groups containing N11 and N22 follows that shown for the group containing N31/N32.

reported for other scorpionate complexes[15,23−26] and toward the lower end of the range observed for dioxomolybdenum(VI) complexes in general (99−114°).[8,39] The Mo1−O1 distances range from 1.895(2) to 1.941(1) Å, with an average of 1.919 Å, and are close to values reported for related Tp^{iPr}-MoO_2(OAr-R) (R = alkyl) complexes (1.866(4)−1.931(2) Å).[25] As is commonly observed for complexes of this type, the Mo atom is considerably closer (ca. 0.78 Å) to the O_3-plane than the N_3-plane associated with the Tp^{iPr} ligand (ca. 1.54 Å) (Table 2).[15,23−26] The molybdenum centers are 0.10−0.16 Å from the mean plane of the equatorial donors, O2, O3, N21, and N31, the displacement being toward the phenolate oxygen atom (Table 2).

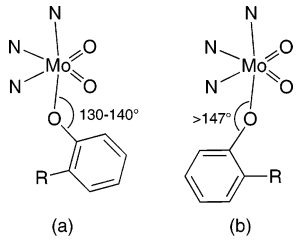

Figure 7. Solid-state structures exhibited by the $^{-}$OAr-R-2 derivatives (only the N donor atoms of Tp^{iPr} shown).

In the solid state, the 2-R-phenolate ligands adopt one of two conformations. In the first (Figure 7a), the phenolate ring is proximal to the terminal oxo ligands and the 2-R group is directed toward a cleft in the Tp^{iPr} ligand, being nestled between the two isopropyl groups on the pyrazolyl groups trans to the oxo ligands. This structure is exhibited by **1** and **12**, as well as the major conformers observed for positionally disordered **2** and **3**. All these molecules have Mo1−O1−C1 angles of ca. 131° except for **2**, where an angle of 138.6(3)° is observed. The ipso ring carbon lies beneath the MoO_2 plane, and the 6-C*H* projects toward and lies in close contact with the oxo ligands (O···*H*C ca. 2.8 Å). In the second coligand conformation (Figure 7b), adopted by **4** and **10** (Supporting Information) and the minor conformers of **2** and **3**, the phenolate ring lies in the Tp^{iPr} ligand cleft and the R-group projects toward the oxo groups. Complexes with this structure are characterized by Mo1−O1−C1 angles greater than 147°, the ipso ring carbon pointing away from the oxo ligands (beneath the equatorial MoN_2 plane). The correlation of Mo1−O1−C1 angle and structure extends to the individual conformers of **2** and **3**. The two *meta*-substituted derivatives **11** and **16** are characterized by the phenolate ring arrangements shown in Figure 7a,b, respectively, but with the substituent pointing away from the Tp^{iPr} ligand in both cases; the Mo1−O1−C1 angles are 134.2(2) and 147.7(2)°, respectively.

The phenolate ring lies close to the pseudo-mirror plane (Mo1,B,N11) in **1**, **3**, **10**, and **12** but is displaced considerably from the pseudo-mirror plane in **2**, **4**, **11**, and **16**; relevant dihedral and Mo1−O1−C1−C2 torsion angles are provided in Table 2.

The Mo1−N21 and Mo1−N31 distances lie in the ranges 2.314(3)−2.350(2) and 2.290(2)−2.338(2) Å, respectively, being longer than the Mo1−N11 distances of 2.186(2)−2.205(2) Å due to the trans influence of the oxo ligands.

Summary

This paper describes the synthesis, characterization, and structural analysis of Tp^{iPr}MoO_2(OAr-R) complexes containing hydrogen-bond acceptors or donors on the phenolate coligand ($^{-}$OAr-R). They represent dioxo−Mo(VI) Tp^{iPr} complexes with the potential for conversion into isolable aqua− or hydroxo−oxo−Mo(V,IV) complexes, with the Tp^{iPr} inhibiting dinucleation and the R group positioned appropriately to stabilize the aqua/hydroxo ligands through hydrogen bonding. Attempts to access such complexes are currently underway.

Acknowledgment. We thank Ms. Sally Duck (Monash University) for mass spectrometric data and Dr. Brendan F. Abrahams for assistance with crystallographic studies and gratefully acknowledge the financial support from the Australian Research Council and the donors of the Petroleum Research Fund (administered by the American Chemical Society).

Supporting Information Available: Detailed ^{1}H and ^{13}C NMR assignments (selected compounds), full listings of IR data (all compounds), the preliminary crystal structure of **10**, ORTEP projections for complexes not shown in the text, and crystallographic data in CIF format. This material is available free of charge via the Internet at http://pubs.acs.org.

IC701957B